Differential regulation of antiviral T-cell immunity results in stable CD8+ but declining CD4+ T-cell memory

DIRK HOMANN[1], LUC TEYTON[2] & MICHAEL B.A. OLDSTONE[1]

[1]*Division of Virology, Department of Neuropharmacology and*
[2]*Department of Immunology, The Scripps Research Institute, La Jolla, California, USA*
Correspondence should be addressed to D.H.; email: dhomann@scripps.edu

Emerging evidence indicates that CD8+ and CD4+ T-cell immunity is differentially regulated. Here we have delineated differences and commonalities among antiviral T-cell responses by enumeration and functional profiling of eight specific CD8+ and CD4+ T-cell populations during primary, memory and recall responses. A high degree of coordinate regulation among all specific T-cell populations stood out against an approximately 20-fold lower peak expansion and prolonged contraction phase of specific CD4+ T-cell populations. Surprisingly, although CD8+ T-cell memory was stably maintained for life, levels of specific CD4+ memory T cells gradually declined. However, this decay, which seemed to result from less efficient rescue from apoptosis, did not affect functionality of surviving virus-specific CD4+ T cells. Our results indicate that CD4+ T-cell memory might become limiting under physiological conditions and that conditions precipitating CD4+ T-cell loss might compromise protective immunity even in the presence of unimpaired CD8+ T-cell responses.

The hallmarks of specific T-cell immunity include proliferative expansion, acquisition of effector function and memory—the long-term maintenance of qualitatively distinct T cells at increased frequencies[1]. In most viral infections, virus-specific CD8+ T cells play a central part through two principal effector pathways: cytolysis and cytokine production[2–5]. Specific CD4+ T cells, additionally required for control of many infections[6–8], contribute to viral clearance through a variety of mechanisms including help for CD8+ and B-cell responses, effector cytokine production and cytolysis. In addition to their functional heterogeneity, emerging evidence indicates that respective regulation of CD8+ and CD4+ T-cell responses is fundamentally different; the distinguishing feature being the presence of oligoclonal CD8+ but not CD4+ T-cell expansions in healthy individuals[9]. Postulated reasons for reduced clonal expansions of CD4+ T cells include smaller burst size and shorter duration in acute immune responses, as well as less efficient rescue from apoptosis and differential homeostatic proliferation in the memory phase[10]. Analyzing these differences is important for understanding protective T-cell immunity and developing prophylactic and therapeutic vaccinations.

Here we performed a contemporaneous and longitudinal evaluation of antiviral CD8+ and CD4+ T-cell responses under conditions of optimal immunity; we used an infectious agent (lymphocytic choriomeningitis virus, LCMV) that is effectively controlled by a mouse host. Our data provide evidence of a highly coordinated, focused and synchronized functional development of epitope-specific CD8+ and CD4+ T-cell populations during both primary and recall responses. However, in contrast to stable CD8+ T-cell memory, specific CD4+ T-cell memory gradually declined. Although this decay was not associated with loss of function among surviving CD4+ T cells, their enhanced susceptibility to apoptosis was indicated by reduced expression of Bcl-2 and Bcl-x_L.

Identification of virus-specific CD8+ and CD4+ T cells

The introduction of major histocompatibility complex (MHC) class I–peptide complexes for identification and enumeration of specific CD8+ T cells has demonstrated a previously unrecognized magnitude of virus-specific CD8+ T-cell responses[11–13]. These observations have stimulated speculation that proliferation-assay–based calculations of virus-specific CD4+ T-cell frequencies have been similarly underrated[14–17]. Recent functional analyses, including those of HIV- and cytomegalovirus (CMV)-specific CD4+ T cells, have indicated significantly higher numbers[8,16,18–22]. However, in the absence of specific MHC class II–peptide reagents, it is still unclear whether these results accurately reflect specific CD4+ T-cell frequencies.

C57BL/6 mice generate LCMV-specific T-cell responses that recognize six different epitopes derived from the viral glycoprotein (GP) or nucleoprotein (NP) restricted by MHC class I (D^b or K^b), and two epitopes restricted by MHC class II (IA^b)[11,18,23] (Table 1). In addition to MHC class I-tetramers[12,13], we have generated class II-tetramers[24,25] for function-independent identification and *ex vivo* phenotyping of epitope-specific T cells. Even at the height of the T-cell response (day 8), less than 10% of specific CD4+ and CD8+ T cells expressed the early activation marker CD69, indicating that most virus-specific T cells had no recent contact with viral antigen (Fig. 1*a*). As observed for specific CD8+ T cells[11], there was a strong correlation between MHC class II-tetramer staining and interferon (IFN)-γ production by specific CD4+ T cells (Fig. 1*b*). These data demonstrate the functionality of MHC class II-tetramers and validate the use of intracellular IFN-γ staining as an accurate assay for enumeration of LCMV-specific CD4+ T cells.

Differential regulation of CD8+ and CD4+ T-cell immunity

T-cell responses can be divided into the three phases of expansion/activation, contraction/death and maintenance/memory[1]. At the peak of the primary T-cell response, approximately 7×10^7 CD8+ T cells in the spleen were specific for LCMV (~1/3 of all splenocytes). In agreement with earlier findings[11] and extended to include all known subdominant epitopes, the distribution of epi-

Table 1 MHC class I- and II- restricted LCMV epitopes

LCMV epitope	Sequence	MHC restriction
GP_{33-41}	KAVYNFATC	D^b/K^b
GP_{34-43}	AVYNFATCGI	K^b
$GP_{276-286}$	SGVENPGGYCL	D^b
$GP_{118-125}$	ISHNFCNL	K^b
GP_{92-101}	CSANNAHHYI	D^b
$NP_{396-404}$	FQPQNGQFI	D^b
$NP_{205-212}$	YTVKYPNL	K^b
GP_{61-80}	GLNGPDIYKGVYQFKSVEFD	I-A^b
$NP_{309-328}$	SGEGWPYIACRTSVVGRAWE	I-A^b

GP: glycoprotein; NP: nucleoprotein.

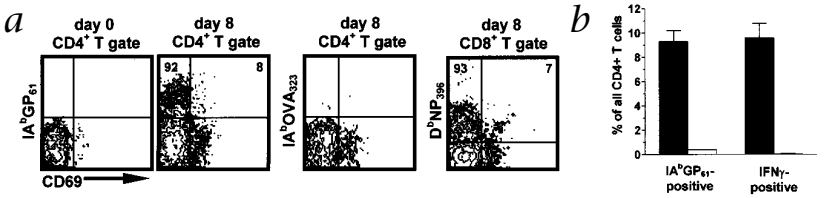

Fig. 1 Identification of virus-specific T cells. ***a***, Detection of epitope-specific T cells with MHC class II–peptide and class I–peptide tetramers. The first and third panels demonstrate the specificity of class II tetramer staining tested on uninfected (IA^bGP_{61}, day 0) or infected (IA^bOVA_{323}, day 8) mice. Dot blots are gated on live (propidium iodide-negative) $CD4^+/B220^-$ T cells or live $CD8^+$ T cells. Values indicate the relative expression of the early activation marker CD69 among epitope-specific $CD4^+$ or $CD8^+$ T cells. ***b***, Correlation of specific MHC class II tetramer binding and IFN-γ production. Splenocytes from virus-infected (day 8, ■) or uninfected (□) mice were stained directly *ex vivo* with IA^bGP_{61} tetramers or were restimulated with GP_{61} peptide and stained for intracellular IFN-γ. Values represent mean ± 1 s.e. of 4–8 mice tested.

tope hierarchies among specific $CD8^+$ T-cell populations established during the initial phase of the immune response remained constant throughout contraction and memory phases (Fig. 2*b* and *c*). Moreover, our results demonstrate stable $CD8^+$ T-cell memory for virtually the entire host lifetime. In comparison, the $CD4^+$ T-cell response, peaking 10 days after virus challenge with approximately 3.5×10^6 specific cells per spleen, was approximately 20-fold smaller (Fig. 2*a*). The ensuing contraction phase of specific $CD4^+$ T-cell populations was delayed as shown by temporary reduction of the specific $CD8^+$:$CD4^+$ T-cell ratio. However, virus-specific $CD4^+$ T-cell memory was never stabilized and steadily decreasing $CD4^+$ T-cell counts led to a subsequent continuous increase of the $CD8^+$:$CD4^+$ ratio (Fig. 3*a*). Throughout this decline, relative sizes of epitope-specific memory $CD4^+$ T-cell pools remained constant (with ~2/3 of the virus-specific $CD4^+$ T-cell response directed against the GP_{61} and ~1/3 against the NP_{309} epitope). The progressive loss of $CD4^+$ T cells could roughly be divided into three phases: during the extended contraction phase between days 15 and 45 there was an exponential decay of specific $CD4^+$ memory T cells with relatively short population half-lives ($t_{1/2}$ GP_{61} = 17.4 d; $t_{1/2}$ NP_{309} = 17.9 d) followed by a transitional phase characterized by progressive increase of population half-lives. Beyond day 180, extended population half-lives remained stable (403–417 d; Fig. 3*b*).

The burst size of specific T-cell responses has been proposed to determine the extent of memory[26]. After attaining stable memory levels on day 25, all epitope-specific $CD8^+$ T-cell populations were found at 6–11% of their burst sizes. At the same time, specific $CD4^+$ T cells were present at 19% (NP_{309}) to 27% (GP_{61}) of their burst sizes due to the delayed contraction kinetics. We calculated that memory T-cell levels comparable to $CD8^+$ T cells, that is, approximately 5–10% of burst size, are reached around day 50 (10%) to day 75 (5%) at which time the specific $CD4^+$ T-cell loss is progressively slowed. Our findings thus indicate that in the absence of further infections, levels of memory cells at 5–10% of the burst size, in spite of continually declining $CD4^+$ T cells, represent an important 'set-point' for virus-specific T-cell memory.

Scope and focus of specific T-cell responses

To directly visualize T-cell expansion during the primary response,

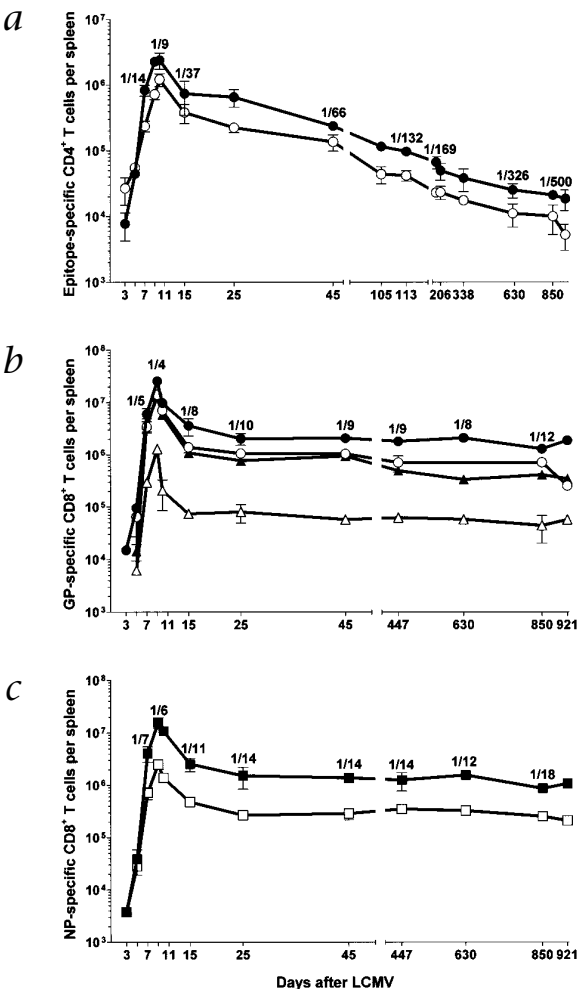

Fig. 2 Enumeration of epitope-specific $CD4^+$ and $CD8^+$ T cells from activation into lifetime memory. Splenocytes were obtained at indicated time points after LCMV infection and peptide-restimulated T cells were analyzed for presence of all epitope-specific T cells by intracellular cytokine staining. At selected time points, staining with MHC class I or class II tetrameric complexes and ELISPOT analyses were performed in parallel. ***a***, Total numbers of GP_{61}- (●) and NP_{309}- (○) specific $CD4^+$ T cells per spleen. ***b***, Total numbers of GP_{33}- (●), GP_{118}- (○), GP_{276}- (▲) and GP_{92}- (△) specific $CD8^+$ T cells per spleen. ***c***, Total numbers of NP_{396}- (■) and NP_{205}- (□) specific $CD8^+$ T cells per spleen. Fractions indicate frequencies of immunodominant GP_{61}-specific $CD4^+$ among all $CD4^+$ T cells and frequencies of GP_{33}- or NP_{396}-specific $CD8^+$ among all $CD8^+$ T cells. Values represent mean ± 1 s.e. of 4–8 mice at all time points with the exception of day 921 for which only 2 mice were available.

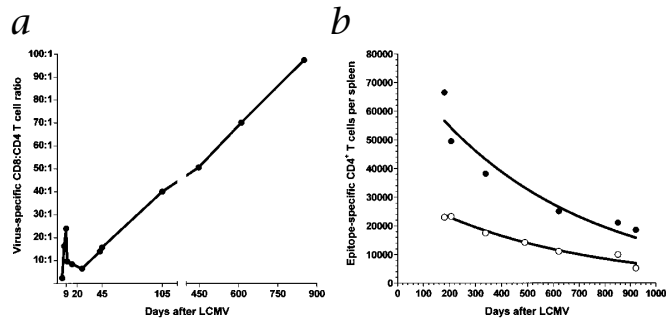

Fig. 3 Decay of specific CD4⁺ T-cell memory. ***a***, Kinetics of specific CD8:CD4 T-cell ratio. To derive the virus-specific CD8:CD4 T-cell ratio in the spleen, the sum of all epitope-specific CD8⁺ T cells (GP_{33}, GP_{276}, GP_{118}, GP_{92}, NP_{396}, NP_{205}) was divided by the sum of epitope-specific CD4⁺ T cells (GP_{61}, NP_{309}). ***b***, Defined decline of epitope-specific CD4⁺ memory T cells. The progressive decline of virus-specific memory CD4⁺ T cells in the spleens of LCMV-immune mice between days 180 and 921 post-infection followed an exponential association. Population half-lives were $t_{1/2}$ = 403 days for GP_{61}-specific CD4⁺ T cells and $t_{1/2}$ = 417 d for NP_{309}-specific CD4⁺ T cells. GP_{61}, (●); NP_{309}, (○).

we determined the extent of bromodeoxyuridine (BrdU) incorporation by proliferating CD8⁺ and CD4⁺ T cells. Over 90% of the CD8⁺ and approximately 50% of the CD4⁺ T cells proliferated during the first nine days of virus infection. As shown previously for CD8⁺ T cells[11], all virus-specific CD8⁺ and CD4⁺ T cells proliferated in response to the virus (data not shown). The extent of specific, antigen-driven proliferation in combination with the relative size of the T-cell response (Fig. 4) allowed us to assess the scope to which our analysis of epitope-specific T cells covers the complete LCMV-specific T-cell response. We calculated that the six MHC class I-restricted CD8⁺ populations accounted for almost the entire antigen-driven CD8⁺ T-cell proliferation. Similar calculations made for the CD4⁺ T-cell response showed that our analysis of just two MHC class II-restricted epitopes covered more than 80% of the CD4⁺ T-cell response. These results emphasize the breadth of our epitope-specific analyses and rule out a major role for bystander activation in both CD8⁺ and CD4⁺ T-cell compartments.

Coordinate functional maturation of T-cell responses

Analysis of the six different MHC class I-restricted T-cell populations at the height of the CD8⁺ T-cell response (~day 8) indicated that up to 75% of the CD8⁺ T cells were virus-specific (Fig. 4). Parallel analyses of the CD4⁺ T-cell response revealed a virus-specific T-cell expansion that comprised at its peak (~day 10) up to 20% of total CD4⁺ T cells. There was a synchronized functional maturation of virtually all epitope-specific T-cell populations as shown by a gradual shift from predominantly IFN-γ–producing effector T cells during the early immune response to simultaneous IFN-γ and tumor-necrosis factor (TNF)-α production by memory T cells. The characteristic IFN-γ⁺/TNF-α⁺ memory phenotype was established around day 30 and maintained indefinitely (that is, until the latest time point tested: 921 days post-infection). *Ex vivo* functional profiling of aged memory cells thus demonstrated preservation of functional T-cell capacities.

Fig. 4 Coordinate regulation of antiviral T-cell responses irrespective of immunodominant determinants and T-cell lineage. Single-cell suspensions obtained from spleen at indicated time points following LCMV infection were restimulated with indicated MHC class I- and II-restricted peptides followed by CD8 or CD4 surface and intracellular IFN-γ and TNF-α staining. Dot blots are gated on CD8⁺ or CD4⁺ T cells; IFN-γ expression (vertical axis) is displayed versus TNF-α expression (horizontal axis). Each row represents the evolution of the indicated epitope-specific T-cell population followed from days 0 through 447. Each column represents the distribution of an individual mouse's T-cell response among the 6 CD8⁺ (GP_{33}, GP_{276}, GP_{118}, GP_{92}, NP_{396} and NP_{205}) and 2 CD4⁺ T-cell epitopes (GP_{61} and NP_{309}). The sum of all IFN-γ⁺ and TNF-α⁺ CD8⁺ or CD4⁺ T cells at a given time point equals the relative magnitude of the virus-specific T-cell response (percent virus-specific T cells).

Unimpaired functionality of aged CD4⁺ memory T cells

To further investigate whether the CD4⁺ T-cell loss is associated with functional impairment of surviving T cells, we evaluated the recruitment kinetics of specific memory CD4⁺ T cells by determining IFN-γ production as a function of *in vitro* restimulation time, and we observed no significant slowing of response kinetics in late (day 206) compared with early (day 45) memory populations (Fig. 5*a*). Old CD4⁺ memory T cells produced even more IFN-γ at the single-cell level, a possible consequence of age-associated changes in cytokine production[27] (Fig. 5*b*). Finally, we measured function-based avidities of specific CD4⁺ T-cell populations by peptide titration. Avidities (defined as peptide concentration required to induce IFN-γ production in 50% of a specific population) of old GP_{61}-specific CD4⁺ memory T-cell populations (day 206: 69 ± 1 nM) were virtually identical to those of GP_{61}-specific effectors (day 8: 75 ± 9 nM). The absence of 'avidity maturation' during the memory phase was further supported by concurrent analyses of Vβ T-cell receptor (TCR) repertoires that demonstrated stable distribution of Vβ usage by specific CD4⁺ T cells from effector phase to long-term memory (data not shown).

Differential regulation of CD8⁺ and CD4⁺ T-cell apoptosis

Survival of memory T cells is the result of a complex balance between pro- and anti-apoptotic factors. The anti-apoptotic function of Bcl-2, a prototypic member of the Bcl-2 family of cell-death regulators, has been shown by rapid loss of peripheral lymphocytes in

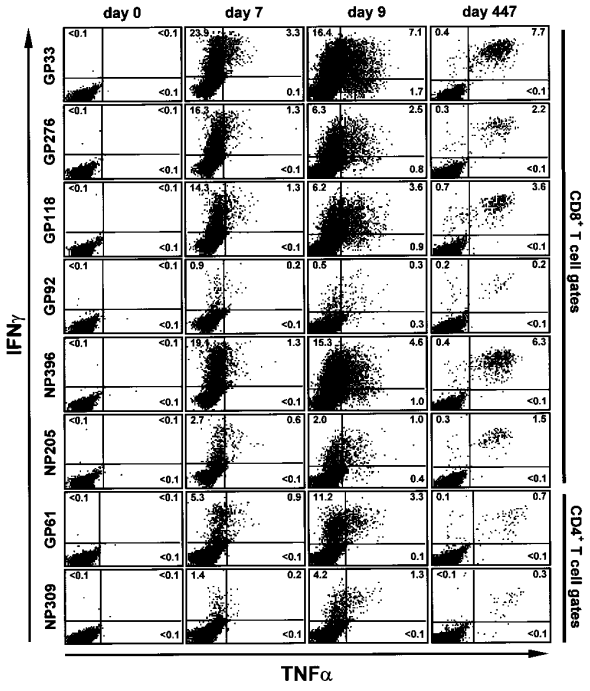

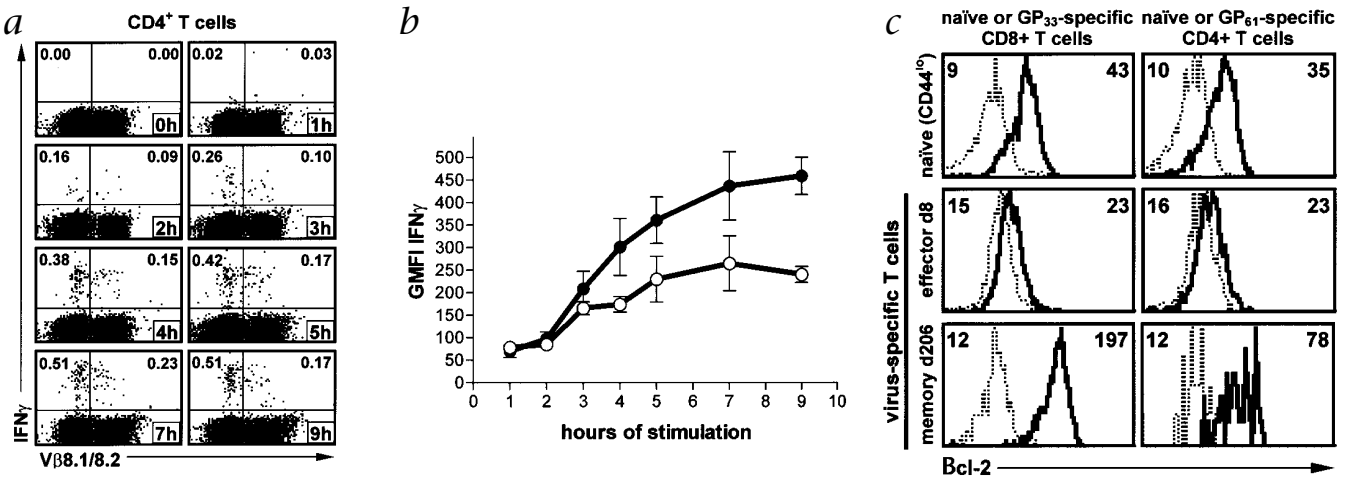

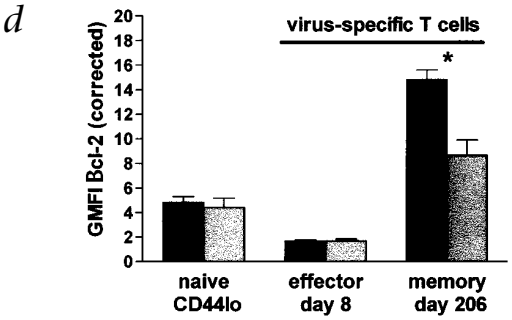

Fig. 5 Functionality of specific CD4+ T cells and apoptosis regulation. ***a***, Recruitment kinetics of virus-specific memory CD4+ T cells. Kinetics of IFN-γ production by specific memory CD4+ T cells (day 206) was visualized by restimulation of immune spleen cells with GP_{61} peptide and determination of intracellular IFN-γ content 0–9 h later as indicated. All panels are gated on CD4+ T cells. ***b***, Semi-quantitative analysis of IFN-γ production at the single-cell level. To determine the amount of IFN-γ produced at the single-cell level, the geometric means of fluorescence intensity (GMFI) of antibody against IFN-γ was evaluated in early (day 45, ○) and late (day 206, ●) GP_{61}-specific memory CD4+ T cells as a function of the duration of *in vitro* restimulation. Values represent mean ± 1 s.e. of 3 mice analyzed. ***c***, Differential Bcl-2 expression by naive, effector and memory CD8+ and CD4+ T cells. Splenic T cells from naive (day 0), effector (day 8) or memory mice (day 206) were analyzed for Bcl-2 expression. Histograms are gated on naive ($CD44^{Lo}$) CD8+ or CD4+ T cells (upper panels) and GP_{33}-specific CD8+ or GP_{61}-specific CD4+ effector and memory T cells (middle and lower panels). Upper right values indicate GMFI of Bcl-2 expression, upper left values GMFI of isotype control. Bcl-2 staining (—); isotype control (- -). ***d***, Reduced Bcl-2 expression by epitope-specific CD4+ memory T cells. For a direct comparison of Bcl-2 expression by CD8+ (■) and CD4+ (■) T cells, the GMFI of Bcl-2 expression in naive ($CD44^{Lo}$) or virus-specific CD8+ (GP_{33}) and CD4+ (GP_{61}) T cells at indicated time points was divided by the GMFI of corresponding isotype stain. The corrected values (mean ± 1 s.e.; 3–5 mice per group) are shown and are representative for 5 independent experiments. *, $P = 0.0144$, Student's *t*-test.

Bcl-2–deficient mice as well as prevention of apoptosis by Bcl-2 overexpression[28]. Naive CD8+ and CD4+ T cells of undefined specificity expressed basal Bcl-2 levels, whereas virus-specific effector T cells demonstrated reduced Bcl-2 expression in agreement with the subsequent demise of most effector cells during the contraction phase (Fig. 5*c*). Like specific memory CD8+ T cells, surviving memory CD4+ T cells expressed elevated Bcl-2 levels as compared with naive and effector cells. However, epitope-specific memory CD4+ T cells showed consistently lower Bcl-2 levels than specific CD8+ T cells (Fig. 5*c* and *d*), a difference that was also noted for NP_{309}-specific CD4+ and NP_{396}-specific CD8+ T cells. Moreover, specific memory CD4+ T cells (day 206) demonstrated a concomitant reduction of the anti-apoptotic Bcl-2 family member Bcl-x_L (geometric mean of fluorescent intensity (GMFI) of Bcl-x_L: 32.7 ± 0.5 for GP_{61}-specific CD4+ and 47.2 ± 1.7 for GP_{33}-specific CD8+ T cells; $P = 0.0013$).

Similarity of specific primary and secondary T-cell responses

To evaluate the proliferative and functional potential of aged memory cells *in vivo*, we performed a direct comparison of primary and secondary T-cell responses. The data in Fig. 2*a–c* allowed us to estimate the 'speed' of specific CD8+ and CD4+ T-cell turnover during the primary immune response. Between days 3 and 9, there was an approximately 3,000-fold increase of GP_{33}- and NP_{396}-specific CD8+ T cells (11–12 divisions). The average doubling time between days 5 and 7 was approximately 6–10 hours for all epitope-specific CD8+ T-cell populations and slowed down to 24–36 hours between days 7 and 9, comparable to recent estimates[11]. The antigen-driven proliferative response of CD4+ T cells was less pronounced. An approximately 550-fold increase of GP_{61}-specific CD4+ T cells between days 3 and 9 was the result of approximately 9 cell divisions. Average division rates for virus-specific CD4+ T cells were 9–20 hours between days 5 and 7, decelerating to 20–40 hours between days 7 and 9. Thus, the 'speed' of the CD4+ T-cell response was slower but comparable in degree to that of CD8+ T cells.

To assess the recall response of virus-specific memory T cells, LCMV-immune splenocytes obtained approximately 1.5 years after primary infection were labeled with CFSE (carboxyfluoroscein diacetate succinimidyl diester) and transferred into congenic recipients followed by high-dose LCMV challenge. By 66 hours after rechallenge, most virus-specific T cells (70–90% of all CD8+ and CD4+ T to be recruited by day 6) had proceeded through one or more cell cycles (Fig. 6*a*). Moreover, the average division rate of proliferating T cells was comparable between CD8+ (21–22 h) and CD4+ (18–19 h) T cells and doubling rates of the fastest dividing CD8+ and CD4+ populations (9.4 h) did not exceed the proliferation rates observed in the primary response. By day 6 after rechallenge (Fig. 6*b*), virtually all epitope-specific T cells had undergone multiple cell divisions. Although virus was rapidly cleared (within 3–4 d), the scope of the proliferative T-cell response was nearly identical to the primary challenge (Fig. 6*c*).

Discussion

In this study we have examined commonalities and differences be-

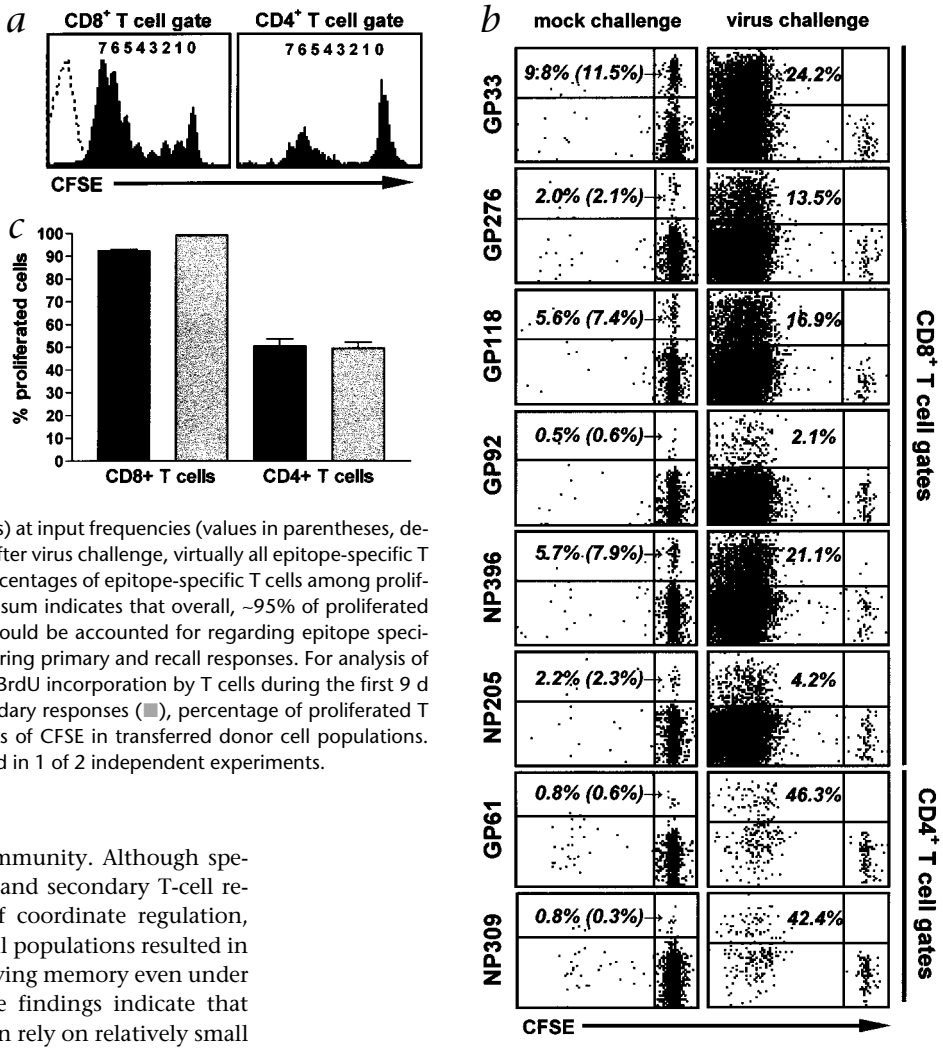

Fig. 6 Coordinate regulation and complete mobilization of aged memory T cells during recall responses. LCMV-immune splenocytes (Thy1.2) obtained ~18 mo after infection were labeled with CFSE and transferred into non-irradiated, congeneic recipients (Thy1.1) followed by high-dose virus challenge. ***a***, Histograms are gated on donor (Thy1.2) $CD8^+$ (left) or $CD4^+$ (right) T cells. Proliferation of donor T cells 3 d (66h) after transfer and challenge is indicated by sequential loss of CFSE fluorescence intensity. Values indicate number of divisions starting with non-divided cells (0 divisions). Dotted line indicates CFSE-negative host T cells. Results were from 3 mice per group. ***b***, Dot blots (IFN-γ versus CFSE) are gated on donor peptide-restimulated $CD8^+$ or $CD4^+$ T cells. Left column: 6 d after transfer, mock-challenged recipients retained epitope-specific donor cells (indicated percentages) at input frequencies (values in parentheses, determined prior to transfer). Right column: 6 d after virus challenge, virtually all epitope-specific T cells had undergone at least 7 cell divisions. Percentages of epitope-specific T cells among proliferated, CFSE-negative cells are specified; their sum indicates that overall, ~95% of proliferated $CD8^+$ and ~92% of proliferated $CD4^+$ T cells could be accounted for regarding epitope specificity. ***c***, Similar extent of T-cell proliferation during primary and recall responses. For analysis of proliferation following primary challenge (■), BrdU incorporation by T cells during the first 9 d following infection was determined. For secondary responses (■), percentage of proliferated T cells was assessed 6 d after rechallenge by loss of CFSE in transferred donor cell populations. Values indicate mean ± 1 s.e. of 3–4 mice tested in 1 of 2 independent experiments.

tween antiviral $CD8^+$ and $CD4^+$ T-cell immunity. Although specific $CD8^+$ and $CD4^+$ as well as primary and secondary T-cell responses demonstrated a high degree of coordinate regulation, differential kinetics of specific $CD4^+$ T-cell populations resulted in smaller responses and progressively decaying memory even under conditions of optimal immunity. These findings indicate that $CD4^+$-dependent protective immunity can rely on relatively small memory populations but is also exposed to potential impairment under conditions of precipitated $CD4^+$ T-cell loss (for example, HIV infection, cancer and old age).

We have delineated differences between $CD8^+$ and $CD4^+$ T-cell immunity in the three phases of activation, contraction and memory. The burst size of the virus-specific $CD8^+$ T-cell response was approximately 20 times larger than that of specific $CD4^+$ T cells. Differential costimulation requirements[7] as well as limited expression of MHC class II versus ubiquitous expression of class I might contribute to the observed differences. The demise of specific $CD4^+$ T cells during the subsequent contraction phase was delayed. Although most effector T cells are thought to die by activation-induced cell death[29], the precise mechanisms remain unclear. Interestingly, a critical step for reaching homeostatic balance seems to be efficient removal of specific T cells by the liver[30], a mechanism that might be particular for activated $CD8^+$ T cells[31] and thus could explain the slowed contraction of specific $CD4^+$ T-cell pools. Also, $CD4^+$ T-cell immunity appears compromised in B-cell–deficient mice[32,33] indicating that specific interactions with B cells could defer $CD4^+$ T-cell removal from lymphoid organs.

An emerging consensus indicates that long-term $CD8^+$ and $CD4^+$ T-cell memory does not require persisting antigen[26,34–37]. However, our use of a replicating infectious agent, although by all accounts completely eliminated[1,34], cannot categorically rule out the persistence of antigen[38] and persisting viruses might induce increased frequencies or impaired functionality and clonal deletion of specific T cells[13]. Among the relatively few animal studies that have investigated maintenance of virus-specific $CD4^+$ T-cell memory over time, several have found comparatively stable $CD4^+$ memory to both readily eliminated (influenza[14] and LCMV (refs. 17,18)) and persistent (γ-herpes[16]) viruses. Although two longitudinal studies showed a decrease of $CD4^+$ memory, the reduction was only temporary and not compared with $CD8^+$ memory[15], or not evaluated in late memory or expanded to memory $CD4^+$ T cells of different epitope specificities[19]. Moreover, a preferential decline of HIV-specific memory $CD4^+$ T cells was noted in subjects with long-term highly active antiretroviral therapy (HAART)-mediated viral suppression[21]. However, this phenomenon was not unique for $CD4^+$ T cells as a similar decline was also observed for HIV-specific $CD8^+$ T cells after HAART (ref. 39). Although our study was not designed to resolve the issue of antigen persistence and memory, it presents evidence for divergent conservation of T-cell memory in the same microenvironment, that is, the stable maintenance of $CD8^+$ memory contrasting with waning $CD4^+$ memory within the same lymphatic organs. Taken together, small burst size and epitope-independent progressive decline of specific $CD4^+$ T-cell populations might contribute to the scarcity of oligoclonal $CD4^+$ populations observed in healthy individuals[9,10].

Maintaining specific T-cell memory is a dynamic balance between longevity of resting cells, homeostatic proliferation and

programmed cell death[40]. Surprisingly, homeostatic proliferation rates were independent of immunodominant determinants, MHC-restriction and age (D.H., unpublished observations) indicating that differential apoptosis regulation might be a factor in memory CD4+ T-cell loss. Similar to virus-specific CD8+ T cells[41], differential Bcl-2 expression by naive (basal), effector (low) and memory (high) CD4+ T cells corresponds to basal, reduced and increased population survival, respectively. Increased Bcl-2 expression by memory CD4+ T cells is not revealed by analysis of CD44^{Hi} CD4+ T cells due to a wide range of Bcl-2 expression indicative of considerable heterogeneity among this T-cell subset (data not shown and ref. 41). Nevertheless, a direct comparison of specific CD8+ and CD4+ T cells demonstrated that elevated Bcl-2 as well as Bcl-x_L levels of memory CD8+ T cells consistently and significantly exceeded those of CD4+ T cells. Thus, reduced levels of 'survival factors' in CD4+ T cells might lead to less efficient rescue from apoptosis and gradual loss of CD4+ memory.

Although numerically vast, the acute LCMV-specific T-cell response is tightly focused. In agreement with other reports, we have obtained no evidence for significant bystander activation of CD8+ T cells[11]. Our analyses also exclude a major role for bystander activation in the CD4+ compartment. In addition to its non-dissipative nature, the virus-specific T-cell response demonstrated a highly coordinated functional regulation from effector to memory phase as shown by shifting T-cell cytokine profiles. Although essential elements of this functional maturation have been noted earlier[42], we report here both the functional evolution of epitope-specific CD8+ T-cell populations independent of immunodominant determinants and the synchronized maturation of epitope-specific CD4+ T-cell responses. Moreover, the characteristic IFN-γ+/TNF-α+ double-positive cytokine profile[8,42] was maintained for life by all surviving memory T cells. Similar to virus-specific CD8+ T cells (ref. 42 and D.H., unpublished data), recruitment kinetics and avidities of specific CD4+ memory T cells were comparable to effector populations of the same specificity. Corresponding *in vivo* data confirmed that aged CD4+ and CD8+ memory T cells retained their capacity to rapidly respond to a rechallenge and mediate accelerated virus control. Increased precursor frequencies of specific T cells with committed effector functions are the cardinal element of this 'accelerated' response since both the overall extent and speed of proliferation were nearly identical to the primary response. Average division times of 6–10 hours observed in the primary response—prompting comparison of T cells with germinal center B cells—likely pose a physiological limit that could not be exceeded by even the fastest-dividing populations during the secondary response. Finally, proliferation of virtually all specific memory T cells indicates that 'secondary memory' is the direct progeny of secondary effector T cells. The latter findings extend the recently proposed linear development of 'primary' CD8+ T-cell memory[43] to 'secondary memory' following rechallenge as well as to the CD4+ compartment. Overall, the pronounced similarities of CD8+ and CD4+ T regulation in both primary and secondary response might reflect common evolutionary roots in the innate inflammatory response[44].

In conclusion, our data indicate that immunization at an early age generates life-long CD8+ but progressively waning CD4+ T-cell immunity. The selective loss of specific CD4+ T cells might require intermittent stimuli such as exposure to antigen or booster vaccinations to rescue CD4+ T cells and maintain complete immunity over long periods of time. Conversely, conditions precipitating CD4+ T-cell loss such as HIV infection[45] might compromise immunity in spite of specific CD8+ T-cell maintenance.

Methods

Mice. C57BL/6 ($D^bK^bIA^b$; Thy1.2) and congenic ($D^bK^bIA^b$; Thy1.1) mice were obtained from the Rodent Breeding Colony at The Scripps Research Institute and housed under specific pathogen-free conditions.

Virus. The Armstrong strain of LCMV, clone 53b, was used throughout all experiments. LCMV was plaque-purified 3 times on Vero cells and stocks prepared by a single passage on BHK-21 cells. 8–12-wk-old mice were infected with a single intraperitoneal (i.p.) dose of 1×10^5 plaque-forming units (p.f.u.). For secondary challenge, mice were inoculated with 10^6 p.f.u. LCMV i.p.

Antibodies. For flow cytometry and ELISPOT assays, we used the following fluorescein isothiocyanate (FITC), phycoerythrin (PE), CyChrome, peridinin chlorophyll-a protein (PerCP) or allophycocyanin (APC) conjugated, biotinylated and/or purified antibodies (PharMingen, La Jolla, California): CD4 (RM4-5), CD8a (53-6.7), CD40L (MR1), CD44 (IM7), CD69 (H1.2F3), CD45R/B220 (RA3-6B2), Vβ-8.1/8.2 (MR5-2), Thy1.2 (53-2.1), IL-2 (JES6-5H4), IFN-γ (R4-6A2, XMG1.2) and TNF-α (MP6-XT22). For 5- and 6-color flow cytometry, CD8a (53-6.7) and CD4 (H129.19) Red613-conjugates (Gibco, Carlsbad, California) as well as Streptavidin-PharRed (PharMingen) were used .

MHC class I and II tetramers. D^bGP_{33}, D^bNP_{396}, D^bGP_{276} and K^bGP_{34} tetramers were obtained as APC- or PE-conjugates from the Tetramer Core Facility, Emory University, Atlanta, Georgia. In some cases, biotinylated MHC–peptide monomers were tetramerized immediately before use. Staining with MHC class I tetramers was performed at a 1:50–1:100 dilution in the presence of various surface antibodies for 30 min at 4 °C. K^bGP_{34} tetramers were used in conjunction with the CT-CD8a clone (Caltag, Burlingame, California) to minimize crossreactivity between reagents. Since the GP_{33-41} peptide is also recognized in the context of K^b (ref. 23), CD8+T cell frequencies obtained with GP_{33} peptide in functional assays roughly correspond to the sum of D^bGP_{33}- and K^bGP_{34}-specific CD8+T cell frequencies (D.H., unpublished observation).Construction, expression, purification and tetramerization of IA^b tetramers presenting tethered LCMV peptides and control IA^b tetramers displaying the $ovalbumin_{323–339}$ epitope were performed as described for IA^{g7} tetramers[24]. Staining was performed in a 0.1% BSA/0.1% NaH_3 PBS buffer for 90 min at 37 °C. Various surface antibodies as well as antibodies against CD4 and B220-CyChrome or -PerCP were added for the final 30 min. Propidium iodide was added at a final concentration of 5 μg/ml to allow analytical exclusion of dead and B cells in the same channel.

Flow cytometry and cytokine ELISPOT. Single-cell suspensions obtained from lymphatic organs were restimulated for 5 h with 1 μg/ml MHC class I-restricted (PeptidoGenic, Livermore, California) or 2 μg/ml MHC class II-restricted (Chiron, Clayton Victoria, Australia) viral peptides in the presence of 10–50 U/ml recombinant human IL-2 (PharMingen) and 1 μg/ml brefeldin A (Sigma). Staining of cell-surface antigen and intracellular antigens was performed as described[8]. Negative controls were peptide-restimulated cells obtained from uninfected mice, cells restimulated for 5 h in the absence of viral peptides and cells stained with conjugated cytokine-specific antibodies preincubated for 30 min at 4 °C with an excess of recombinant cytokine. Cells were acquired with FACSort or FACSCalibur flow cytometers (Beckton Dickinson, San Jose, California) using Cell Quest software (Beckton Dickinson). For 5- and 6-color analyses, a FACSVantage SE flow cytometer (Beckton Dickinson) was used. ELISPOT assays were performed and evaluated as described[8].

***In vivo* proliferation assays using BrdU and CFSE.** A bromodeoxyuridine (BrdU; Sigma) solution of 0.8 mg/ml sterile water was prepared fresh daily and supplied as drinking water for the first 9 d of virus infection. Intracellular detection of BrdU and cytokines in peptide-restimulated T cells was performed using reagents and protocols provided by manufacturer (BrdU flow kit, PharMingen). For CFSE labeling, memory T cells (Thy1.2) were enriched by depletion of B220+ cells using magnetic beads (Dynal, Lake Success, New York). Enriched cell populations were resuspended at a concentration of 1×10^7/ml in prewarmed PBS/0.1% BSA and incubated for 10 min at 37 °C with 1.5 μl of a 5-mM CFSE stock solution (Molecular Probes, Eugene, Oregon). After washing, cells were resuspended in PBS and transferred intravenously into non-irradiated congenic (Thy1.1) recipients followed immediately by

virus or mock challenge. Shortest division times were calculated by dividing time after challenge (66 h) by number of divisions (7) completed by the population with lowest CFSE fluorescence intensity. Mean division time was calculated by adding the products of relative population size (that is, fraction of cells per completed division among all cells that have undergone at least 1 division) and corresponding division time (ranging from 9.4 h for population 7 to 66 h for population 1).

Bcl-2 and Bcl-x_L stains. Bcl-2–specific antibody (3F11) and isotype control (A19-3) were obtained as PE-conjugates and used for intracellular staining according to manufacturer's instructions (PharMingen). The PE-conjugated 7B2.5 antibody was used for specific detection of intracellular Bcl-x_L (Southern Biotechnology Associates, Birmingham, Alabama). This antibody recognizes both human and rodent Bcl-x_L.

Statistical analyses. Data handling, analysis and graphic representation was performed using Prism 2.01 (GraphPad Software, San Diego, California). The exponential decay of specific $CD4^+$ T is described by the association $n = a \times e^{-bt} + c$, where n = number of specific $CD4^+$ T cells in spleen; t = time after virus challenge; and a, b and c = constants with c fixed at $c = 0$.

Acknowledgments

We thank V. Apostolopolous and V. Mallet-Designé for help with MHC class II tetramer preparation and staining; A. Saluk and J. Trotter for assistance with 5- and 6-color flow cytometry; and M. von Herrath, M. Manchester, J. Sprent and I. Abramson for insightful discussions. This work is supported by NIH grants AG-04342 and AI-09484 (to M.B.A.O.) as well as NIH training grant AG-00080 and Juvenile Diabetes Foundation International fellowship 3-1999-629 (to D.H.).

RECEIVED 19 APRIL; ACCEPTED 15 JUNE 2001

1. Ahmed, R. & Gray, D. Immunological memory and protective immunity: Understanding their relation. *Science* **272**, 54–60 (1996).
2. Zinkernagel, R.M. & Doherty, P.C. MHC-restricted cytotoxic T cells: Studies on the biological role of polymorphic major transplantation antigens determining T-cell restriction-specificity, function, and responsiveness. *Adv. Immunol.* **27**, 51–177 (1979).
3. Oldstone, M.B. Immunotherapy for virus infection. *Curr. Top. Microbiol. Immunol.* **134**, 211–229 (1987).
4. Homann, D. Immunocytotherapy. *Curr. Top. Microbiol. Immunol.* (in the press).
5. Guidotti, L.G. & Chisari, F.V. Cytokine-induced viral purging—role in viral pathogenesis. *Curr. Opin. Microbiol.* **2**, 388–391 (1999).
6. Kalams, S.A. & Walker, B.D. The critical need for $CD4^+$ help in maintaining effective cytotoxic T lymphocyte responses. *J. Exp. Med.* **188**, 2199–2204 (1998).
7. Whitmire, J.K. & Ahmed, R. Costimulation in antiviral immunity: differential requirements for $CD4^+$ and $CD8^+$ T-cell responses. *Curr. Opin. Immunol.* **12**, 448–455 (2000).
8. Berger, D.P., Homann, D. & Oldstone, M.B. Defining parameters for successful immunocytotherapy of persistent viral infection. *Virology* **266**, 257–263 (2000).
9. Beverley, P.C. & Maini, M.K. Differences in the regulation of $CD4^+$ and $CD8^+$ T-cell clones during immune responses. *Philos. Trans. R. Soc. Lond. B. Biol. Sci.* **355**, 401–406 (2000).
10. Maini, M.K., Casorati, G., Dellabona, P., Wack, A. & Beverley, P.C. T-cell clonality in immune responses. *Immunol. Today* **20**, 262–266 (1999).
11. Murali-Krishna, K. *et al.* Counting antigen-specific $CD8^+$ T cells: A reevaluation of bystander activation during viral infection. *Immunity* **8**, 177–187 (1998).
12. Doherty, P.C. & Christensen, J.P. Accessing complexity: The dynamics of virus-specific T-cell responses. *Annu. Rev. Immunol.* **18**, 561–592 (2000).
13. Welsh, R.M. Assessing CD8 T-cell number and dysfunction in the presence of antigen. *J. Exp. Med.* **193**, F19–22 (2001).
14. Topham, D.J. *et al.* Quantitative analysis of the influenza virus-specific $CD4^+$ T-cell memory in the absence of B cells and Ig. *J. Immunol.* **157**, 2947–2952 (1996).
15. Topham, D.J. & Doherty, P.C. Longitudinal analysis of the acute Sendai virus-specific $CD4^+$ T-cell response and memory. *J. Immunol.* **161**, 4530–4535 (1998).
16. Christensen, J.P. & Doherty, P.C. Quantitative analysis of the acute and long-term CD4(+) T-cell response to a persistent gammaherpesvirus. *J. Virol.* **73**, 4279–4283 (1999).
17. Varga, S.M. & Welsh, R.M. Stability of virus-specific $CD4^+$ T-cell frequencies from acute infection into long term memory. *J. Immunol.* **161**, 367–374 (1998).
18. Whitmire, J.K., Asano, M.S., Murali-Krishna, K., Suresh, M. & Ahmed, R. Long-term $CD4^+$ Th1 and Th2 memory following acute lymphocytic choriomeningitis virus infection. *J. Virol.* **72**, 8281–8288 (1998).
19. Kamperschroer, C. & Quinn, D.G. Quantification of epitope-specific MHC class-II-restricted T cells following lymphocytic choriomeningitis virus infection. *Cell. Immunol.* **193**, 134–146 (1999).
20. Varga, S.M. & Welsh, R.M. High frequency of virus-specific interleukin-2-producing CD4(+) T cells and Th1 dominance during lymphocytic choriomeningitis virus infection. *J. Virol.* **74**, 4429–4432 (2000).
21. Pitcher, C.J. *et al.* HIV-1–specific $CD4^+$ T cells are detectable in most individuals with active HIV-1 infection, but decline with prolonged viral suppression. *Nature Med.* **5**, 518–525 (1999).
22. Rentenaar, R.J. *et al.* Development of virus-specific CD4(+) T cells during primary cytomegalovirus infection. *J. Clin. Invest.* **105**, 541–548 (2000).
23. Hudrisier, D., Oldstone, M.B. & Gairin, J.E. The signal sequence of lymphocytic choriomeningitis virus contains an immunodominant cytotoxic T-cell epitope that is restricted by both H-2D(b) and H-2K(b) molecules. *Virology.* **234**, 62–73 (1997).
24. Stratmann, T. *et al.* The I-Ag7 MHC class II molecule linked to murine diabetes is a promiscuous peptide binder. *J. Immunol.* **165**, 3214–3225 (2000).
25. Ferlin, W., Glaichenhaus, N. & Mougneau E. Present difficulties and future promise of MHC multimers in autoimmune exploration. *Curr. Opin. Immunol.* **12**, 670–675 (2000).
26. Hou, S., Hyland, L., Ryan, K.W., Portner, A. & Doherty, P.C. Virus-specific $CD8^+$ T-cell memory determined by clonal burst size. *Nature* **369**, 652–654 (1994).
27. Hobbs, M.V. *et al.* Patterns of cytokine gene expression by $CD4^+$ T cells from young and old mice. *J. Immunol.* **150**, 3602–3614 (1993).
28. Chao, D.T. & Korsmeyer, S.J. BCL-2 family: Regulators of cell death. *Annu. Rev. Immunol.* **16**, 395–419 (1998).
29. Lenardo, M. *et al.* Mature T lymphocyte apoptosis—immune regulation in a dynamic and unpredictable antigenic environment. *Annu. Rev. Immunol.* **17**, 221–253 (1999).
30. Belz, G.T., Altman, J.D. & Doherty, P.C. Characteristics of virus-specific $CD8^+$ T cells in the liver during the control and resolution phases of influenza pneumonia. *Proc. Natl. Acad. Sci. USA* **95**, 13812–13817 (1998).
31. Mehal, W.Z., Juedes, A.E. & Crispe, I.N. Selective retention of activated $CD8^+$ T cells by the normal liver. *J. Immunol.* **163**, 3202–3210 (1999).
32. Homann, D. *et al.* Evidence for an underlying $CD4^+$ helper and $CD8^+$ T-cell defect in B-cell–deficient mice: Failure to clear persistent virus infection after adoptive immunotherapy with virus-specific memory cells from μMT/μMT mice. *J. Virol.* **72**, 9208–9216 (1998).
33. van Essen, D., Dullforce, P. & Gray, D. Role of B cells in maintaining helper T-cell memory. *Philos. Trans. R. Soc. Lond. B. Biol. Sci.* **355**, 351–355 (2000).
34. Murali-Krishna, K. *et al.* Persistence of memory $CD8^+$ T cells in MHC class I-deficient mice. *Science* **286**, 1377–1381 (1999).
35. Garcia, S., DiSanto, J. & Stockinger, B. Following the development of a $CD4^+$ T-cell response *in vivo*: From activation to memory formation. *Immunity* **11**, 163–171 (1999).
36. Swain, S.L., Hu, H. & Huston, G. Class II-independent generation of $CD4^+$ memory T cells from effectors. *Science* **286**, 1381–1383 (1999).
37. Goldrath, A.W. & Bevan, M.J. Selecting and maintaining a diverse T-cell repertoire. *Nature* **402**, 255–262 (1999).
38. Ciurea, A. *et al.* Persistence of lymphocytic choriomeningitis virus at very low levels in immune mice. *Proc. Natl. Acad. Sci. USA* **96**, 11964–11969 (1999).
39. Ogg, G.S. *et al.* Quantitation of HIV-1–specific cytotoxic T lymphocytes and plasma load of viral RNA. *Science* **279**, 2103–2106 (1998).
40. Marrack, P. *et al.* Homeostasis of αβ TCR^+ T cells. *Nature Immunol.* **1**, 107–111 (2000).
41. Grayson, J.M., Zajac, A.J., Altman, J.D. & Ahmed, R. Increased expression of Bcl-2 in antigen-specific memory $CD8^+$ T cells. *J. Immunol.* **164**, 3950–3954 (2000).
42. Slifka, M.K. & Whitton, J.L. Activated and memory $CD8^+$ T cells can be distinguished by their cytokine profiles and phenotypic markers. *J. Immunol.* **164**, 208–216 (2000).
43. Opferman, J.T., Ober, B.T. & Ashton-Rickardt, P.G. Linear differentiation of cytotoxic effectors into memory T lymphocytes. *Science* **283**, 1745–1748 (1999).
44. Fearon, D.T. & Locksley, R.M. The instructive role of innate immunity in the acquired immune response. *Science* **272**, 50–53 (1996).
45. McCune, J.M. The dynamics of $CD4^+$ T-cell depletion in HIV disease. *Nature* **410**, 974–979 (2001).